Freezing transition of xenon on graphite: A computer-simulation study

S. W. Koch* and Farid F. Abraham
IBM Research Laboratory, San Jose, California 95193
(Received 16 August 1982)

The freezing transition of xenon adsorbed on graphite at high coverage and temperature is studied by constant-pressure and constant-area molecular dynamics. The transition is found to be first order, in contrast to a recent x-ray-diffraction experiment [P. A. Heiney *et al.*, Phys. Rev. Lett. 48, 104 (1982)]. Also, recent objections for using computer experiments to study the melting transition [A. Novaco and P. Shea, Phys. Rev. B 26, 284 (1982) and S. Toxvaerd (unpublished)] are shown to be invalid for the two-dimensional Lennard-Jones system.

I. INTRODUCTION

Over the past decade, the study of phase transitions of physisorbed systems has gained the attention of a large number of experimentalists and theorists in the physics and chemistry communities. Numerous novel innovations in experimental surface science has led to the discovery of a vast richness of adsorption phenomena at solid surfaces, which have, in turn, stimulated a great deal of theoretical activity in the study of the phases of *quasi-two-dimensional* systems, such as rare gases on graphite.[1] Computer simulation has added a new dimension to the scientific investigation of this field, as evidenced by the great variety of computer experiments which have established the important features of the phase diagram for two-dimensional simple atomic systems.[2] An obvious next step is to study, by the simulation approach, the phases of the quasi-two-dimensional systems, and pioneering efforts have been made in this direction (e.g., see Refs. 3 and 4).

In this study we investigate the freezing transition of xenon adsorbed on graphite at high coverage and temperature by employing the constant-pressure and constant-area molecular dynamics simulation techniques. The transition is found to be first order, in contrast to a recent x-ray-diffraction experiment. But before we discuss the xenon-graphite experiments, we present the essential requisites for understanding the simulation details. Also, evidence is presented for the validity of using computer experiments for studying phase transitions, in answer to some misgivings of certain researchers.

II. COMPUTER MODEL AND NUMERICAL SIMULATION METHOD FOR STUDYING XENON ON GRAPHITE

A. Potentials of interaction

We have adopted the well-known Lennard-Jones 6-12 pair potential,

$$\varphi(r)=4\epsilon\left[\left[\frac{\sigma}{r}\right]^{12}-\left[\frac{\sigma}{r}\right]^{6}\right], \tag{2.1}$$

to represent the van der Waals interaction between the various atoms of the xenon-graphite system. The parameters ϵ and σ are determined empirically. We take the xenon-xenon parameters[5] to be $\epsilon/k=225.3$ K and $\sigma=4.07$ Å and the xenon-carbon parameters[6] to be $\epsilon/k=79.5$ K and $\sigma=3.74$ Å.

The total potential energy U for a given configuration of N xenon atoms $r(i)$, $i=1,\ldots,N$, above a *fixed* configuration of carbon atoms defining the graphite semi-infinite solid $R(j)$, $j=1,\ldots,\infty$, has the form

$$U=\sum_{i>j}^{N}\varphi_{\text{Xe-Xe}}(\,|r(i)-r(j)|\,)+\sum_{\substack{i=1\\(\text{Xe})}}\sum_{\substack{j=1\\(\text{C})}}\varphi_{\text{Xe-C}}(\,|r(i)-R(j)|\,), \tag{2.2}$$

where simple pair-wise additivity of the interatomic interactions is assumed.

In order to reduce computational time in the evaluation of the potentail energy, certain approximations and procedures were implemented. The xenon-xenon potential is truncated at 3σ. Furthermore, Hockney's *chainlink* method is employed so

more, Hockney's *chainlink* method is employed so that the tests for locating atoms within 3σ of any subset of the total number N of the xenon atoms.[7]

The xenon-atom—graphite-substrate interaction may be evaluated analytically by expanding this potential as a Fourier sum in the surface reciprocal-lattice vectors.[6] While the analytical expression is useful for many applications, its use in computer simulations can be very costly in terms of computer time because of the occurrence of sums over trigonometric and exponential functions. To overcome this difficulty, we use a fast and efficient algorithm recently proposed by Dion *et al.*[8] The algorithm breaks up the semi-infinite graphite solid into three regions (see Fig. 1). Region I is the surface layer and its contribution to the atom-substrate potential is obtained by explicitly summing over some subset A of the surface atoms and integrating over the rest. The first few underlayers comprise region II, and their contribution is obtained by integrating over each layer. The remainder of the graphite solid is region III, and its contribution is approximated as a single integral. We take 36 atoms in subset A of region I and three layers for region II, this being sufficient to reproduce Steele's results[6] for the xenon-graphite potential.[7] For the majority of our simulations, we neglect the detailed atomic planar structure of the graphite surface, i.e., model the graphite surface as if the atoms are uniformally distributed as a constant-density x-y sheet. In this case we use the Dion algorithm, but simply set the number of carbon atoms in subset A of region I equal to zero.

B. Computational cell geometry

In Fig. 2(a) a schema of the computational cell geometry is presented. The atomic carbon positions of the graphite surface define the x-y plane at $z=0$, which is also the basal plane of the computational box. This base is a parallelogram compatible with the triangular lattice of a close-packed two-dimensional crystal. Periodic boundary conditions are imposed at the four faces of the computational cell which pass through the sides of the basal parallelogram at normal incidence to the surface. In those simulations where the atomic-substrate structure is taken into account, the basal plane of the computational box must be compatible with the graphite structure, otherwise periodic replication creates unphysical size dependencies. The graphite surface structure is shown in Fig. 2(b). It can be constructed by replicating a basic cell with two atoms, the cell's shape being a parallelogram and its x extension "a" equalling 2.46 Å. The x extension of the computational XL cell has to satisfy the relation

$$XL = ma \ , \tag{2.3}$$

where m is a nonzero integer. Thus the possible XL values are very restricted, and the size of the basal plane cannot be varied continuously. In a constant-pressure simulation, XL must be allowed to vary continuously; hence for this case, we neglected the atomic structure of the graphite basal planes described in Sec. II A.

A reflecting wall is placed at the top of the com-

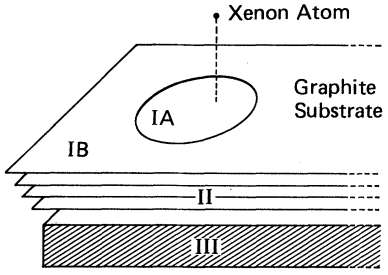

FIG. 1. Model for calculation of graphite-xenon interaction potential. Shown are the three regions summed over in computing the potential: region IA, surface layer, near region; IB surface layer, far region; II, first three underlayers; III, remainder of the solid.

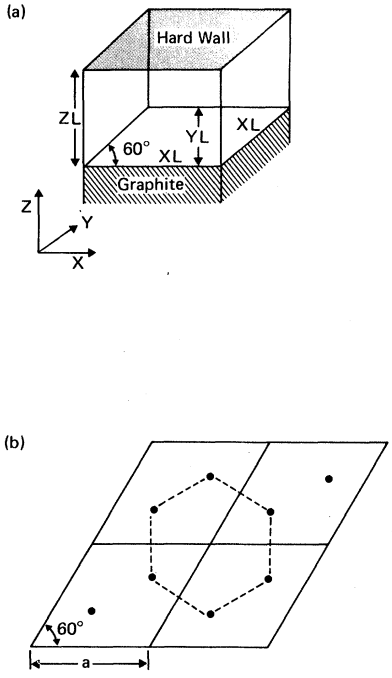

FIG. 2. (a) Geometry of the computational box for the simulation of xenon on graphite. The graphite surface defines the x,y plane at $z=0$. The extensions of the computational box are XL, YL, and ZL, respectively. (b) Structure of the graphite surface. Shown are four graphite unit cells with two carbon atoms per cell (indicated as dots).

putational box, at $z=ZL$. The contact density $\rho(ZL)$ of the xenon fluid at this wall is proportional to the fluid pressure $P(ZL)$ at this wall, where

$$P(ZL)=kT\rho(ZL) . \tag{2.4}$$

In the simulation we set $ZL=2.2\sigma$. This is to be compared with the first- and second-layer mean normal distances from the graphite surface of 0.9σ and 1.84σ, respectively. Also, we show that for a hard-wall distance of 2.2σ the xenon profile is not "distorted" by the presence of the wall.

C. Molecular dynamics simulation method

Simulation techniques of classical statistical mechanics enable one to carry out systematic studies on the structure and energetics of many-particle systems, where only the form of the intermolecular interaction energy is assumed and the external conditions (e.g., temperature and pressure) are specified. Recently, these simulation techniques have been extended to a variety of surface-physics problems associated with physical microclusters, liquid surfaces, liquid-vapor interfaces, and two-dimensional phase transitions, to cite just a few of the growing areas of research.[9] The two main simulation techniques are the Monte Carlo method of Metropolis *et al.*[10] and the molecular dynamics method.[11] For this study we use a new procedure for simulating by molecular dynamics a system under conditions of constant pressure and temperature.[12] Conventional molecular dynamics consists of integrating Newton's equation of motion to obtain the trajectories of the atoms, where the total energy is a constant of the motion as the system evolves along its trajectory in phase space. In the isobaric-isothermal molecular dynamics method the following two changes from the conventional molecular dynamics are adopted: (1) In order to simulate a constant temperature, the atomic velocities are renormalized at every numerical time step, so that the mean kinetic energy corresponds to the specified temperature T; (2) in order to simulate a constant pressure, the volume of the computational cell is changed randomly by ΔV within some prescribed range at every time interval τ_P, requiring the scaling of all the atomic coordinates by an appropriate factor, and with an accompanying total energy change ΔU. Adopting the Metropolis test, if the quantity

$$\Delta W=\Delta U+P\Delta V-NkT\ln\left[1+\frac{\Delta V}{V}\right] \tag{2.5}$$

is negative, this "scaled" configuration is accepted. If it is positive, this configuration is accepted only with the probability equal to $\exp(-\Delta W/kT)$. The time evolution is still governed by the numerical integration of the classical equations of motion, but with the velocity renormalization and position being periodically performed at the specified time intervals. To describe this molecular dynamics method succinctly, the stochastic dynamics of the individual atoms in the isobaric-isothermal Monte Carlo method is replaced by the deterministic equations of motion with the added feature of velocity renormalization—everything else remains the same. For equilibrium phases, time averaging of the state variables over a sufficient temporal evolution of the system by this molecular dynamics method will yield the proper isobaric-isothermal ensemble averages.

In our simulations we use a fifth-degree numerical integration scheme (see Ref. 12 for details), and τ_P is taken to equal two time steps. In the volume scaling we allow the area A of the basal plane to fluctuate in size with the constraint that the height of the computational box remains constant. Therefore, the *parallel pressure* $P_{||}$, given by

$$P_{||}=kT\frac{\partial}{\partial V}\ln Q\Big|_{N,T,ZL} , \tag{2.6}$$

is a constant during a simulation, while the *normal pressure* $P_{\perp}$, given by

$$P_{\perp}=kT\frac{\partial}{\partial V}\ln Q\Big|_{N,T,A} , \tag{2.7}$$

fluctuates about is equilibrium mean value which is governed by the physical system. In (2.6) and (2.7), Q is the partition function. The familiar spreading pressure ϕ is simply

$$\phi=(\langle P_{||}A\rangle-\langle P_{\perp}V\rangle)/\langle A\rangle . \tag{2.8}$$

For the simulations in this study the parallel pressure and spreading pressure are almost identical because under the simulation conditions the normal pressure is very small. In the simulations the parallel pressure is also calculated from the virial expression in order to verify its equality with the specified $P_{||}$ used in Eq. (2.5). Typical total simulation times are 30 000 to 40 000 time steps, or 1500—2000 psec for xenon.

III. A PREAMBLE TO THE THREE-DIMENSIONAL SIMULATION: FREEZING IN TWO DIMENSIONS

A perspective on two-dimensional melting and vaporization of the Lennard-Jones system via computer simulation has been recently reported,[12] and we will assume that the reader is familiar with its contents. We feel that it is particularly important to emphasize the unique advantages gained in perform-

ing constant-pressure computer experiments when addressing the issue of the character of the phase transition. Two-phase coexistence associated with the existence of a first-order phase transition may occur when the mean density of the system is constrained to be constant and may lead an investigator to conclude that the *average* properties of the total system suggest a peculiar phase of matter. This situation cannot occur in a constant-pressure experiment since two-phase coexistence is not thermodynamically allowed. Another advantage is that the discontinuities in density and enthalpy for a first-order transition are directly observed in the experiment. These points are discussed and demonstrated in great detail in Ref. 12. There are some new aspects of our two-dimensional simulations that have not been previously published and which we feel are relevant to this present study.

A. Long relaxation times in the phase-transition region?

Very recently, Novaco and Shea[13] have questioned the usefulness of doing computer-simulation experiments to determine the nature of the two-dimensional melting transition. They conclude that, for a system of atoms interacting through an r^{-5} repulsive interaction and near the phase transition, the system's behavior is characterized by both increasing relaxation times and increasing "thermodynamic" fluctuations, no true metastable states are observed, and this "critical slowing down" behavior supports the view that the transition is continuous. (The quotes are ours.) In their text, they castigate the computer-simulation practitioner for using some "rule of thumb" or qualitative criterion for ascertaining the existence of equilibrium for a particular experiment. (The quotes are theirs.) Well, while we

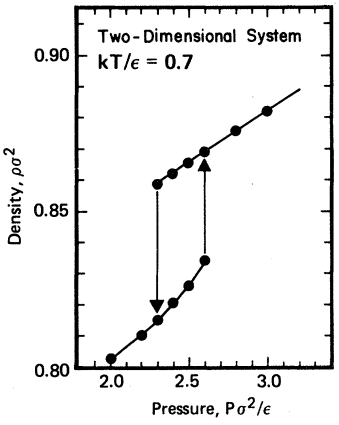

FIG. 3. Equilibrium density vs pressure for a series of constant-pressure simulations of a strictly two-dimensional system. The temperature is $T^*=0.7$.

felt confident that our many stringent tests for equilibrium were sufficient, we definitely felt obligated to apply the Novaco-Shea analysis to our experiments on the Lennard-Jones system. Their analysis consisted of evaluating an autocorrelation function for certain block-averaged thermodynamic variables, e.g., in their constant-energy, *constant-density* simulations, the autocorrelation function is evaluated for a set of block-averaged temperatures $T(i)$, and is given by the relation

$$\langle\langle T(i);T(0)\rangle\rangle=\frac{\langle T(i+n)T(n)\rangle-\langle T(n)\rangle^2}{\langle T(n)T(n)\rangle-\langle T(n)\rangle^2}\ , \tag{3.1}$$

where $\langle\ \rangle$ refers to the average over n. Novaco and Shea find that, in the phase-transition region, the temperature autocorrelation function has a very long relaxation time.

We have applied the Novaco-Shea analysis to constant-temperature, constant-pressure melting simulations of a two-dimensional Lennard-Jones system, the choice of temperatures and pressures being dictated by our eventual interest in comparing these results with our experiments of xenon on graphite (to be discussed in a later section of this paper). We studied various pressures along the isotherm $T^*=kT/\epsilon=0.7$. In Fig. 3 the equilibrim density $\rho^*=\rho\sigma^2$ is presented for a Lennard-Jones system of 576 atoms as a function of pressure $P^*=P\sigma^2/\epsilon$ and for the temperature of 0.7. We note that, for increasing pressures, the equilibrium liquid density increases smoothly up to a pressure of 2.6, at which point the liquid freezes into a solid after 13 000 time steps with a dramatic increase in equilibrium density. Further increase of pressure results in a smooth increase of equilibrium solid density. By sequentially decreasing the pressure and equilibrating the solid, the system passes through $P^*=2.6$ and remains a solid with smoothly decreasing density down to a pressure of 2.4. At $P^*=2.3$, the solid melts after 8000 time steps with a sharp decrease in density. This establishes hysteresis when passing back through the apparent freezing pressure.

In Fig. 4(a) the "block-averaged density" of the system, averaged over each 100 time steps, as a function of time, is presented for $P^*=2.6$, which is the point shown in Fig. 3 where the liquid freezes into a solid. We note the beginning of the crystallization process after 10 000 time steps and its completion after 14 000 time steps. In Fig. 4(b) the Novaco-Shea autocorrelation function of the density is presented for both the *metastable* liquid branch and stable solid branch. Certainly, we are in the *phase-transition region,* as considered by Novaco and Shea, but, in sharp contrast to their findings, we do

not observe a long relaxation time or an increase in "thermodynamic" fluctuations, we observe a true metastable state, we see no evidence for a process of "critical slowing down," and we see a first-order phase transition. In Figs. 5 and 6 we present the time-dependent blocked-averaged density and its respective autocorrelation function for a solid at $P^*=2.5$ (quenched from $P^*=2.6$) and for a liquid at $P^*=2.5$ (quenched from $P^*=2.4$), these two states being bounded by the freezing transition at $P^*=2.6$ and the melting transition at $P^*=2.3$ in Fig. 3. For these single-phase states in the phase-transition region (we emphasize the modifier "single-phase"), we do not see any evidence for a long relaxation-time phenomenon. In Fig. 7 we demonstrate how one might be misled by believing that one can observe a very slow relaxation process simply by doing a constant-density simulation in the two-phase region of solid and liquid. In this figure we show a trajectory analysis of the atomic motions from a constant-energy molecular dynamics simulation of a 576-atom Lennard-Jones system at a fixed density of 0.84 and mean temperature of 0.7, this being directly in the coexistence region.[14] We observe solid-liquid coexistence. Similar to the Novaco-Shea analysis, the block-averaged temperature and its autocorrelation function are presented as a function of time, and we observe what an experimentalist may

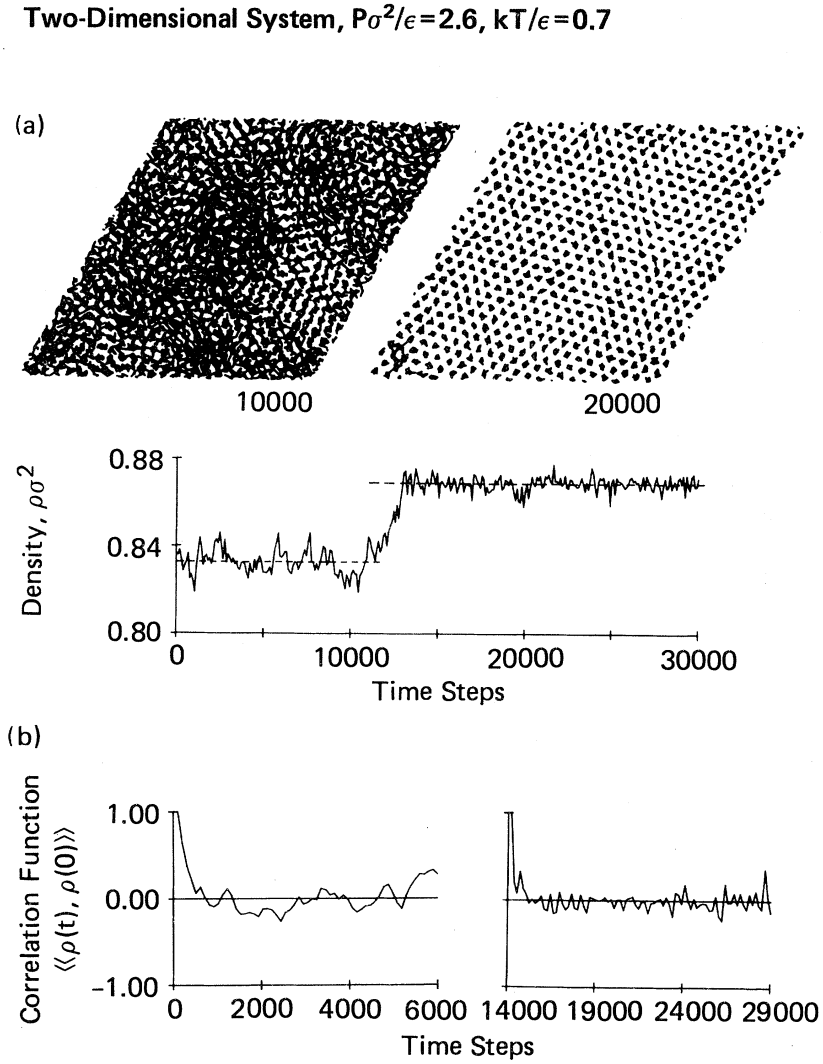

FIG. 4. (a) Trajectory pictures for a two-dimensional system at $P^*=2.6$ which was initialized from a liquid at $P^*=2.5$. The numbers indicate the number of time steps. The blocked-averaged density (averaged over 100 time steps) vs time is also shown. (b) The density autocorrelation function as function of time; the left figure is obtained for the time steps 1–12 000, where the system is in a metastable liquid state, and the right figure is obtained for the time steps 14 000–31 000, where the system is in the equilibrium solid state [see (a)].

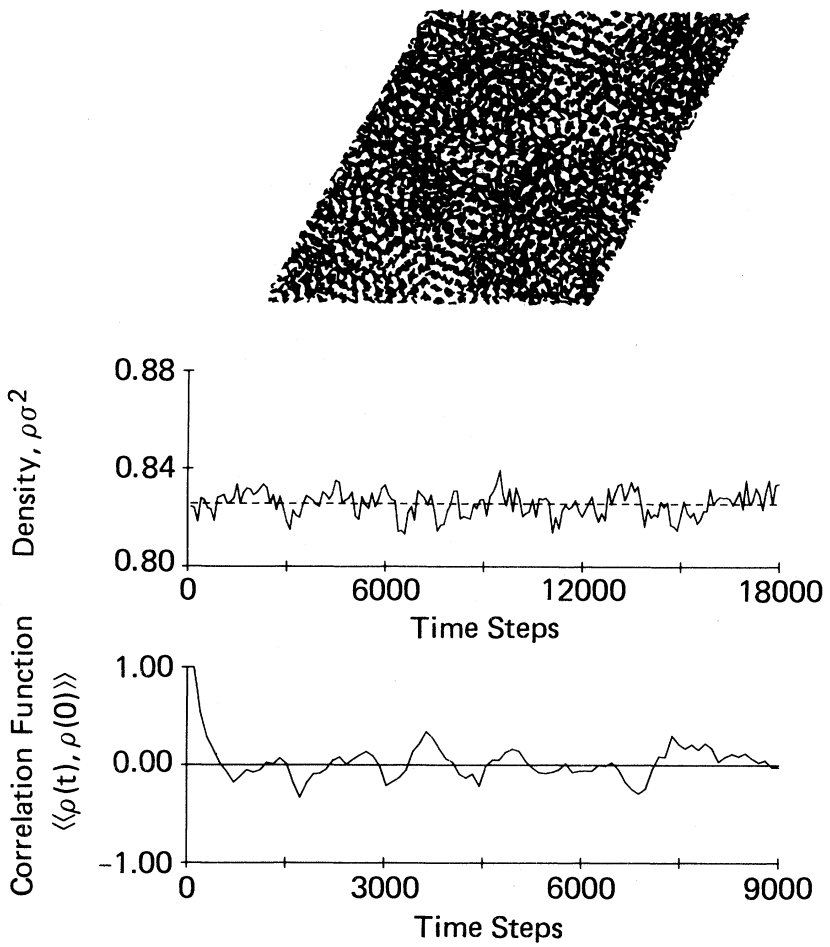

FIG. 5. Trajectory picture, block-averaged density vs time and density autocorrelation function for a two-dimensional liquid at $P^*=2.5$, $T^*=0.7$, which was initialized from a liquid at $P^*=2.4$.

be tempted to interpret as a "nonequilibrium, single-phase phenomenon with a very long relaxation time," if this experimentalist believed that he was measuring a property associated with a single phase. In actual fact, what we are measuring is the fluctuation in time of the ratio of solid to liquid in our simulated system, the fluctuations correlating well with the relative areas of liquid and solid as determined from the time-dependent trajectory pictures.

We conclude that equilibration of a single-phase state, whether stable or metastable, occurs very rapidly in the phase-transition region, contrary to the conclusion of Novaco and Shea. We mention that questions of convergence and accuracy of the Monte Carlo technique may be understood in terms of the dynamics of the appropriate stochastic model, as discussed by Müller-Krumbhaar and Binder.[15]

B. Size effects in the simulation: Do they mislead us?

First, there is the famous Peierls-Landau theoretical demonstration that the atomic *equilbrium* positions in a two-dimensional crystal become uncorrelated at large separations. The quantitative measure for the loss of long-range crystalline order is the difference between the average separation between two atoms and the distance corresponding to the proper number of lattice spacings. It is found that this difference diverges very slowly with the separation distance of the crystalline atoms, the depen-

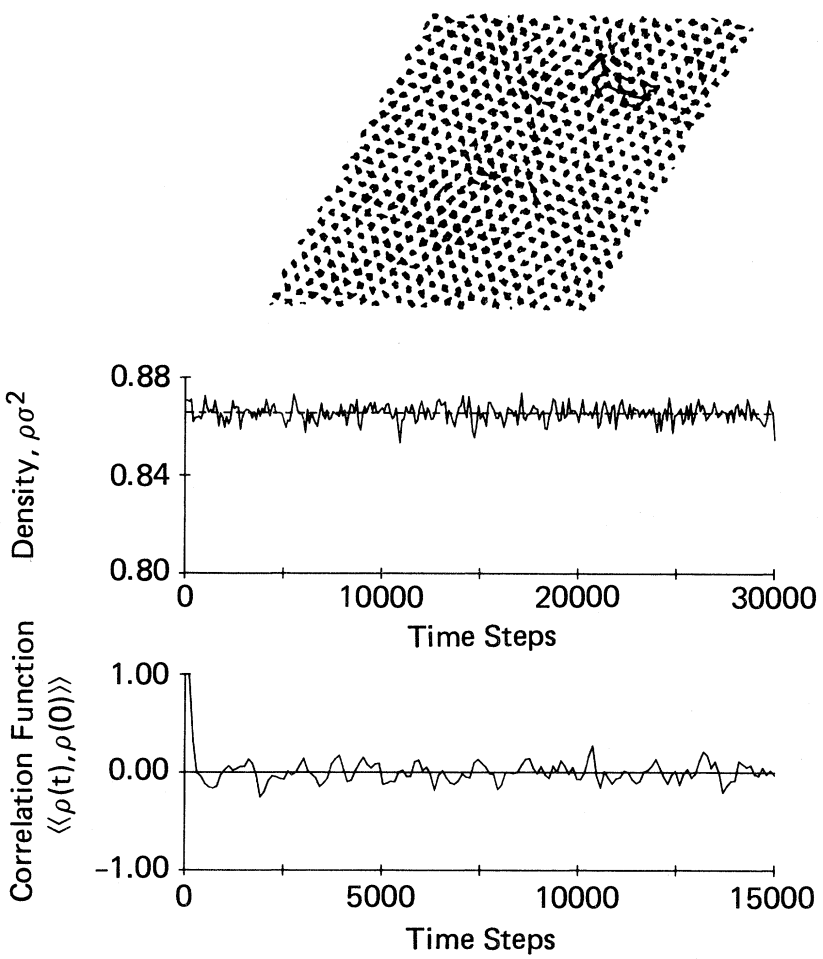

FIG. 6. Same as in Fig. 5, but for a two-dimensional solid at $P^*=2.5$, $T^*=0.7$, which was initialized from a solid at $P^*=2.6$.

dence being only logarithmic. This breakdown of this two-particle correlation also manifests itself in another property; the root-mean-squared displacement θ of a vibrating atom with respect to its mean position diverges logarithmically with crystal size N, as first demonstrated by Hoover[16] and more recently found by Toxvaerd,[17] i.e., letting "b" denote the lattice constant

$$\theta^2=\text{const}\ln N\ , \tag{3.2}$$

where

$$\theta^2=\left\langle\frac{1}{N}\sum_{i=1}^{N}[r(i)-\langle r(i)\rangle]^2\right\rangle\Big/b\ . \tag{3.3}$$

Based on soft-disk simulations, Toxvaerd[17] has recently coupled this feature with the Lindemann stability criterion for the solid state[18] and concludes that there exists a strong number dependence of the location of melting on crystal size; the solid melts if θ is greater than 0.18 of the lattice constant. Furthermore, a questionable interpretation of the simulation results on atomic diffusion leads Toxvaerd to believe that the soft-disk system obeys this new Lindemann's stability criterion and that the first-order nature of two-dimensional melting observed in computer experiments is "wiped out already for systems of 10^4–10^5 particles." However, there is no sound basis for these conclusions, and, in particular, Toxvaerd's application of Eq. (3.2) to Lindemann's criterion is not valid. Lindemann's criterion relates

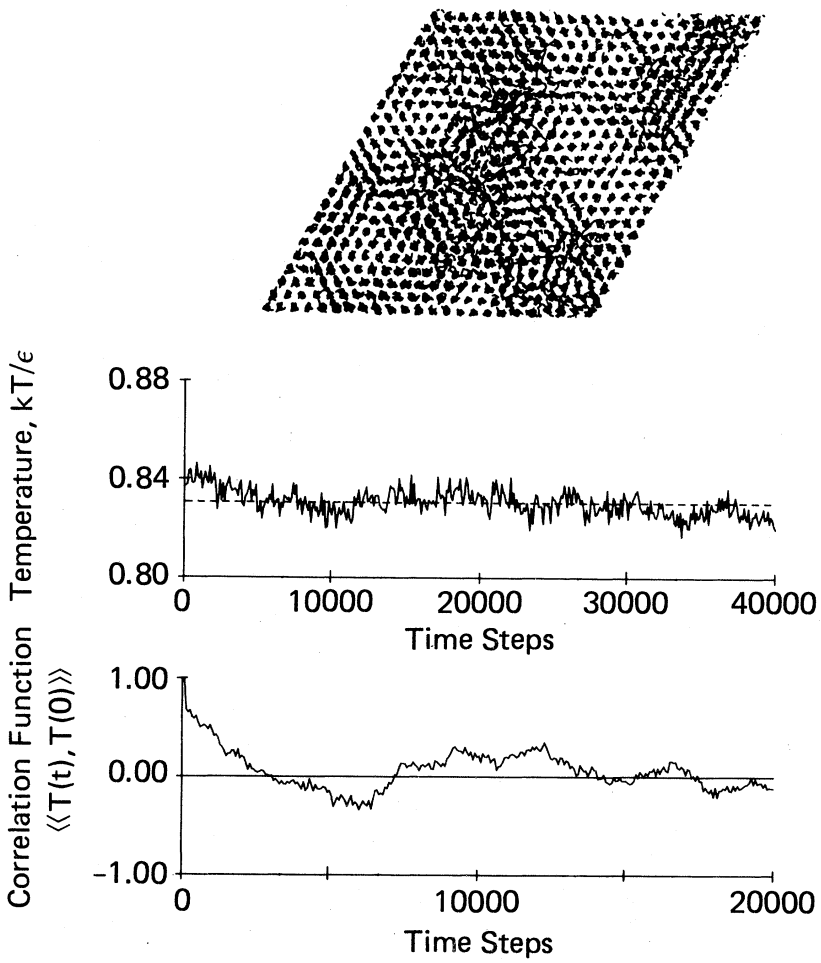

FIG. 7. Trajectory picture, block-averaged temperature vs time and temperature autocorrelation function for a two-dimensional system in a constant "total-energy" simulation at mean temperature $T^*=0.7$ and a density $\rho^*=0.84$. The system shows solid-liquid equilibrium coexistence.

to the mean separation between nearest neighbors, which is obtained from the two-particle correlation function, and not to the mean displacement of an individual particle with respect to its mean position. For two dimensions, this mean nearest-neighbor separation $\bar{a}$, defined in Eq. (3.4), is a constant:

$$\bar{a}=\int_{\text{1st shell}} dr\, r^2 g(r) \Big/ \int_{\text{1st shell}} dr\, r g(r) \qquad (3.4)$$

i.e., it does not diverge logarithmically with crystal size. Both of these features are demonstrated in Fig. 8. Hence, there is no size-dependent melting criterion arising from the application of the Lindemann recipe to a two-dimensional crystal.

We consider a second conclusion arrived at by Toxvaerd: "A system of 8100 particles exhibits melting properties at a point, which should be a stable solid according to previous calculations for a smaller system." This is based on a questionable interpretation of the simulation results on atomic diffusion in the soft-disk solid, and we demonstrate this by simulating the stability of the solid state as a function of system size at the freezing transition of $T^*=0.7$ and $P^*=2.6$ for the Lennard-Jones system. Again, this can only be unambiguous for a constant-pressure experiment where two-phase coexistence cannot occur. In Fig. 9 we note *solid-state stability* for a system of 2304 atoms and for a time of 40 000 time steps, where $d/a>0.18$ and, hence solid-state instability should occur using Toxvaerd's criterion. Also, we note that local mobility fluctua-

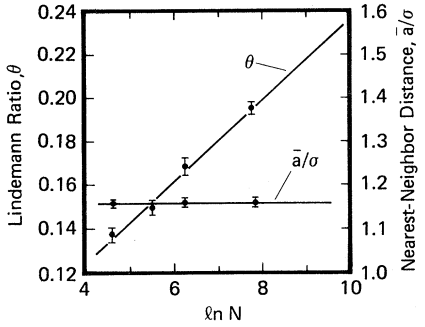

FIG. 8. Lindemann's ratio θ vs $\ln N$, the logarithm of the number N of atoms (left scale) for two-dimensional solids at $P^*=2.6$ and $T^*=0.7$. Also plotted (right scale) is the mean nearest-neighbor distance calculated from the pair distribution function.

tions are prevalent in the *equilibrium* solid.

We have one last comment on the effects of a system's size L on measured results. In Fig. 10 we demonstrate the $1/L$ dependence of the structure factor's first peak width on a system's size for a two-dimensional crystal (e.g., see Ref. 19). For a two-dimensional liquid where the structure of the radial distribution function dies out long before the dimension of the system is reached, there is no system's size dependence for the peak width of the structure factor.

IV. XENON ON GRAPHITE: A SERIES OF MOLECULAR DYNAMICS EXPERIMENTS

Motivated by the recent experimental study by Heiney *et al.*[20] we became interested in investigating any influence of the *third dimension of freedom* on the order of the freezing transition of a *quasi*-two-dimensional liquid. In particular, Heiney *et al.*[20] interpreted their results as indicating the transition to be continuous with fluid correlation lengths exceeding 100 atomic spacings for a coverage of 1.1 monolayers and for a reduced temperature of approximately 0.7. Of course, this is contrary to lower-coverage laboratory experiments, as mentioned in Ref. 20, and to the computer simulations.[12] We have made several simulations in the pressure-

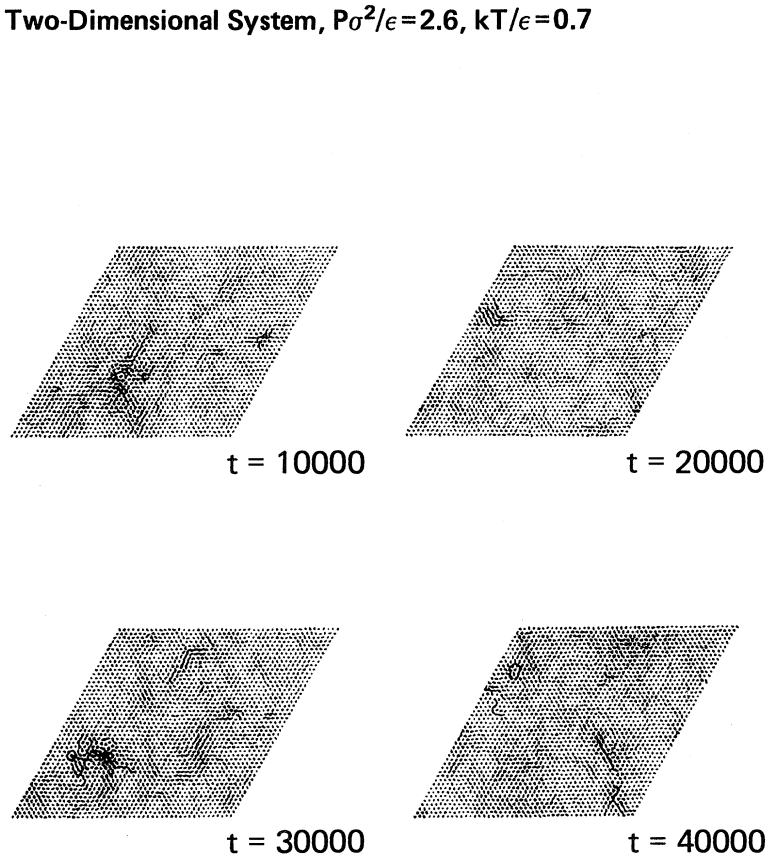

FIG. 9. Time sequence of trajectory plots of a two-dimensional 2304-atom solid which has a $\theta=0.195$. The numbers labeling the plots are the time steps after the initialization in a triangular lattice.

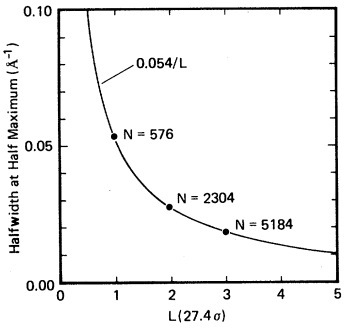

FIG. 10. Halfwidth at half maximum of the first Bragg peak of the atomic structure factor vs the system size L (in units of 27.4σ). The numbers labeling the dots are the number of atoms in the respective two-dimensional constant-pressure simulations at $P^*=3.0$, $T^*=0.7$.

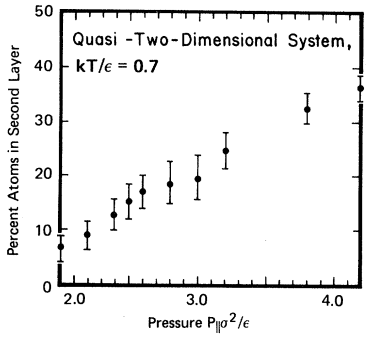

FIG. 12. Percentage of atoms in the second layer vs pressure for the *quasi*-two-dimensional constant-pressure simulations at $T^*=0.7$.

temperature regime where (1) the two-dimensional Lennard-Jones phase diagram predicts a first-order liquid-solid transition, while (2) the laboratory experiment suggests that the high-density liquid freezes in a continuous manner. This section describes the detailed findings of the computer experiments. In the next section, we comment on the laboratory experiments in relation to our simulation findings.

A. Simulations along an isotherm and an isobar

For the isotherm simulations the temperature is fixed at $T^*=0.7$, and a series of constant-pressure simulations are performed for pressures in the range $P^*_{||}=2.0$–4.2, which bound the freezing transition point for this high temperature. The experiments were performed sequentially from the lowest to the highest pressure. Both 576- and 5184-atom systems are studied in order to check for any unusual size dependence. For the 5184-atom system, pressures $P^*_{||}=2.0$, 2.4, 2.5, and 4.2 are examined and, unless stated otherwise, the results agree with the smaller system. The xenon monolayer is initialized as a two-dimensional monolayer at the normal distance $z_m=0.9\sigma$, corresponding to the minimum of the xenon-graphite potential. After equilibrium, 20 000–30 000 time steps are performed typically to obtain the equilibrium properties of the system, such as the enthalpy, number density, atomic distribution functions, and other pertinent quantities. Careful attention is given to determine that the system is in "local equilibrium" (stable or metastable) when taking the statistics for the quantities of interest, e.g., the distribution, running mean, and "autocorrelation" relation of density, enthalpy, and virial pressure are monitored, as well as particle distribution functions and trajectory pictures of the temporal evolution being scrutinized.

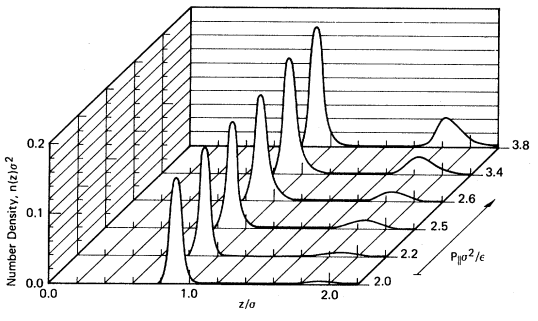

FIG. 11. Number density vs z, the distance from the graphite surface, for the *quasi*-two-dimensional system at various pressures labeling the respective axes.

In Fig. 11 the number-density distribution normal to the graphite substrate $n(z)$ is presented for the denoted pressures and shows two well-defined peaks defining the first and second *layers* of adsorbed xenon centered at approximately z_m and $2z_m$, respectively, which are separated by a very pronounced minimum region. This physical separation allows us to unambiguously define the properties associated with layers 1 and 2, and we take the normal distance separating these two layers at $z=1.4\sigma$. We also note that, with increasing pressure, the peak height of the second layer increases, which simply indicates an increasing population of the second layer with pressure. This is shown quantitatively in Fig. 12, where the percentage of the total number of atoms in the second layer is plotted as a function of pressure, this percentage increasing monotonically from approximately 7% at $P^*_{||}=2.0$ to 36% at $P^*_{||}=4.2$. Furthermore, we note that the change in this distribution function is smooth and suggests no means for determining a change of state for the adsorbed layer. We define the "effective" two-dimensional density for a layer ρ^*_i, $i=1,2$, as the total number of atoms in that

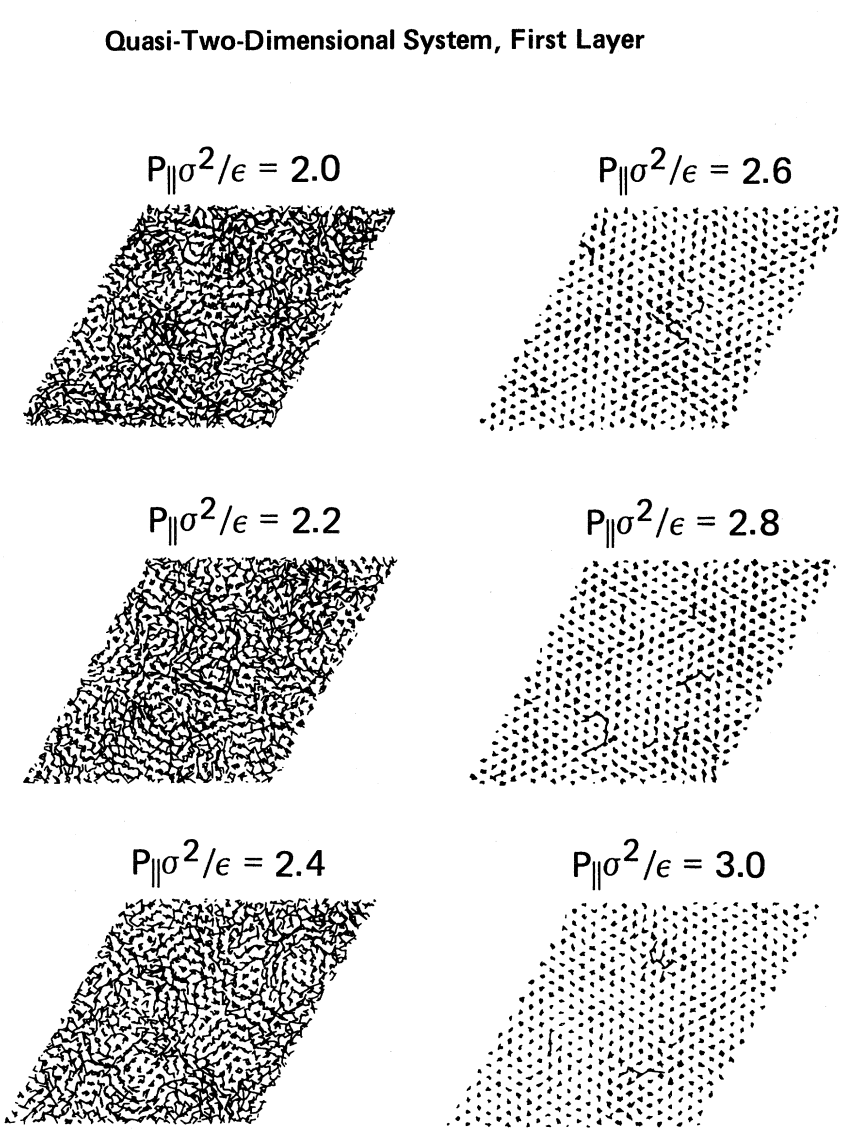

FIG. 13. Trajectory pictures of the equilibrium states in the first layer for the *quasi*-two-dimensional constant-pressure simulations at $T^*=0.7$.

layer divided by the mean cross-sectional area.

Trajectory pictures are a powerful means for determining the states of matter, whether they be solid or liquid, by displaying the temporal evolution in space of the individual atoms during the simulation process. The trajectory of a particular atom is constructed by connecting its x-y positions for a chosen number of time steps. In Figs. 13 and 14 we show examples of trajectory pictures for the equilibrium states of the first and second layers, respectively, at selected pressures. In the first layer we note a transition from the liquid state to the solid state by passing from $P^*_{\|}=2.4$ to $P^*_{\|}=2.6$. This is in contrast to the second layer where the fluid state exists for all pressures because of the low second-layer atomic densities. The temporal evolution of the freezing transition at $P^*_{\|}=2.6$ is presented in Fig. 15, as well as the density variation during freezing. The numbers labeling each picture give the number of time steps after going from an equilibrium liquid configuration for $P^*_{\|}=2.5$. We clearly see the existence of the fluid until 6000 time steps ($\rho^*_1=0.85$), the occurrence of the freezing transition at 8000 time steps, and the completion of solidification after 10 000 time steps ($\rho^*_1=0.88$).

In Fig. 16 the effective two-dimensional density ρ^*_1 is presented as a function of pressure for the first layer. Starting at pressure $P^*_{\|}=2.0$, the xenon layer equilibrates to the liquid state with a mean density of 0.805, evidence for a given state being liquid or

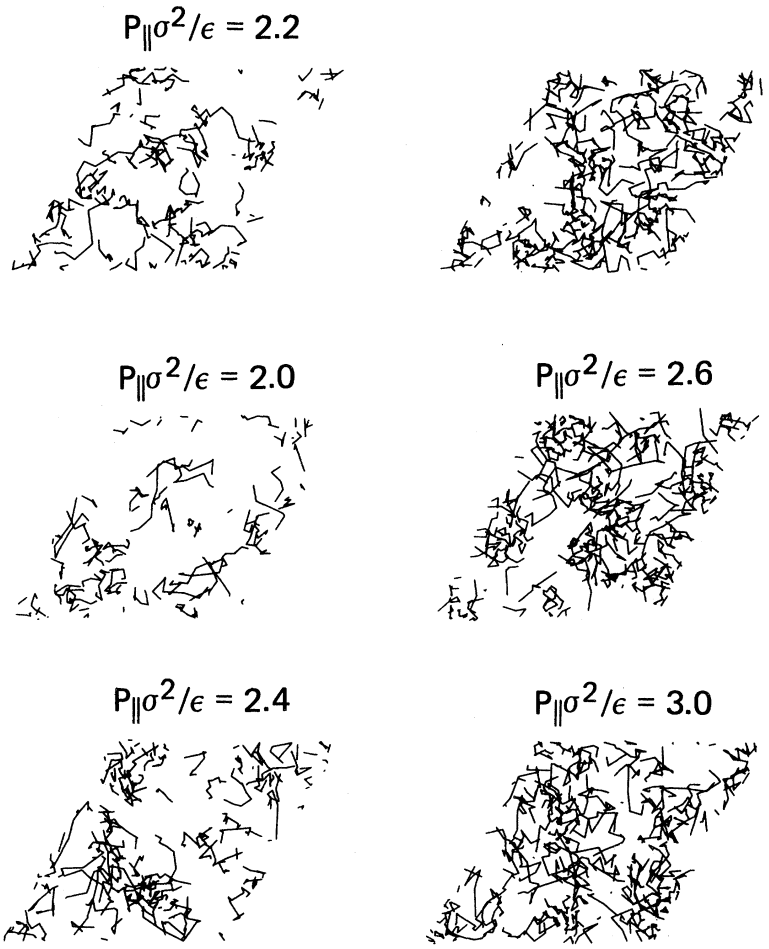

FIG. 14. Trajectory pictures of the equilibrium states in the second layer for the *quasi*-two-dimensional constant-pressure simulations at $T^*=0.7$.

solid being already given from the trajectory pictures. We observe a discontinuous jump in density at $P^*_{||}=2.6$, associated with the first-order freezing transition, and the subsequent solid density increase with increasing pressure. Hysteresis is also demonstrated by sequentially lowering the pressure from an equilibrium solid-state phase, resulting in first-order melting at $P^*_{||}=2.5$ and in a discontinuity in density.

A comparison with the strictly two-dimensional simulations reveals the same qualitative features of the liquid-solid transition for our simple atomic system. However, the two-dimensional densities (Fig. 3) at a given pressure are slightly lower than the effective first-layer densities at the same pressure (Fig. 16), this being a consequence of the finite, though small, width of the atomic distribution $n(z)$ in the first (Fig. 11). This additional "dimension of freedom" also accounts for the reduction of the hysteresis loop in the quasi-two-dimensional system, i.e., it is easier for the adsorbed system to freeze and solidify, in relation to its two-dimensional analog.

The experimental results are found to be quite size independent, when comparing the 576-atom and 5184-atom simulations. However, like the two-dimensional case, there is a pronounced size dependence in the Fourier transform of the radial distribution function (the structure factor) for the solid-state phase (see the latter part of Sec. III B). This is shown in Fig. 17, where the halfwidth at half maximum of the structure factor versus the wave-number position of the maximum is plotted. We ob-

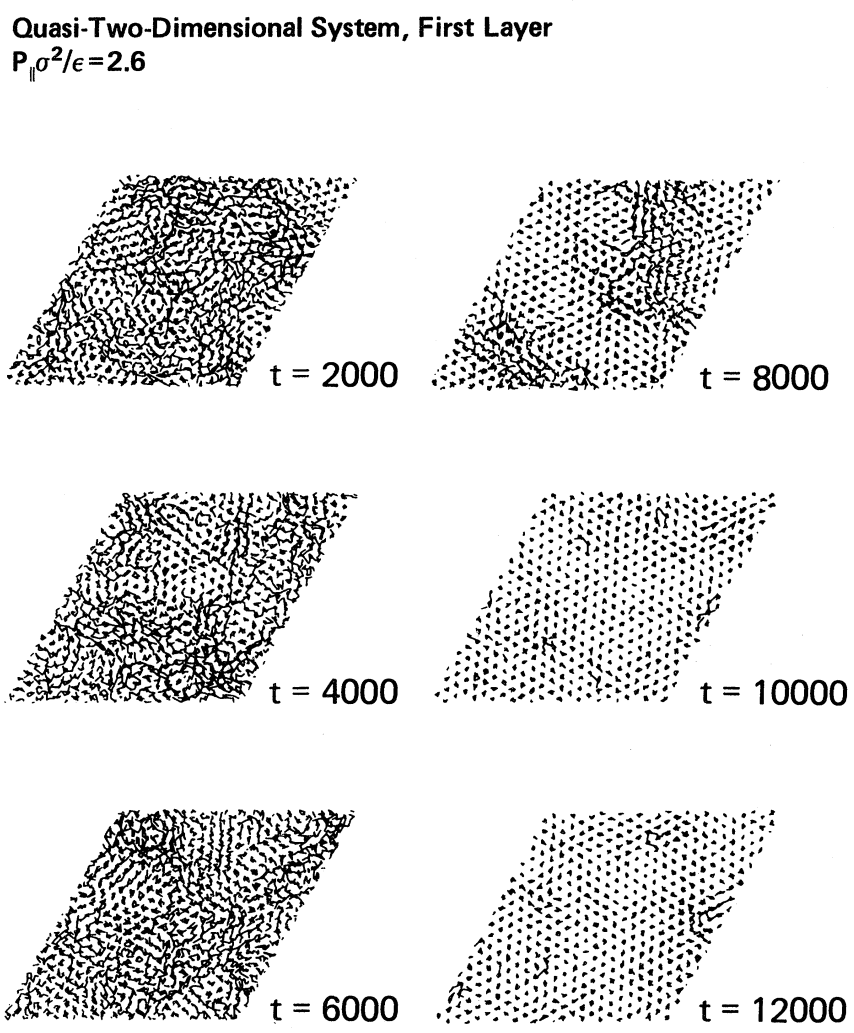

FIG. 15. Trajectory pictures showing the time evolution of freezing in the first layer for the simulation at $T^*=0.7$ and $P^*_{\|}=2.6$. The numbers at the plots are the time steps after the quench from a liquid at $P^*_{\|}=2.5$.

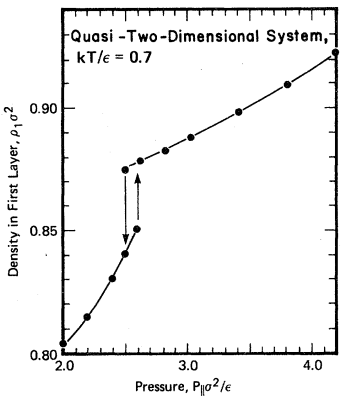

FIG. 16. Effective two-dimensional density in the first layer vs pressure for the *quasi*-two-dimensional constant-pressure simulations at $T^*=0.7$.

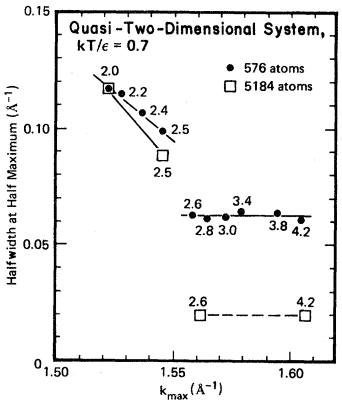

FIG. 17. Halfwidth at half maximum of the first peak of the atomic structure factor vs peak position for various pressures indicated at the points. The dots are for a 576-atom system and the squares for a 5184-atom system.

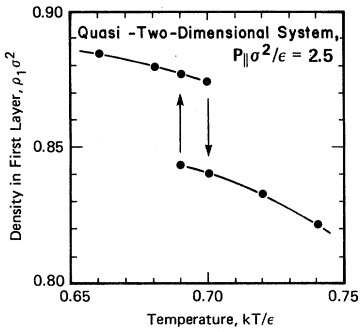

FIG. 18. Effective two-dimensional density in the first layer vs temperature for the *quasi*-two-dimensional constant-pressure simulations at $P^*_{\|}=2.5$.

serve a very broad peak for the liquid states and no significant system-size dependence and, at freezing, we note a discontinuity, the magnitude being directly related to the "$1/L$" dependence of the halfwidth on the size L of the solid system. The halfwidth and peak position are entirely determined by the atoms in the first layer. This is because the second-layer atoms form a low-density fluid with very little structure in the radial distribution function.

We have also performed a series of constant-pressure simulations of xenon on graphite in which the parallel pressure is held fixed at $P^*_{\|}=2.5$ and the temperature is varied over the range of $T^*=0.66$–0.74. Some selected results are summarized in Figs. 18 and 19. In the effective two-dimensional density behavior as a function of temperature, we note that the xenon undergoes freezing at $T^*=0.69$ and solidification at $T^*=0.70$; hence the features of a first-order transition are again measured. Also, the expected behavior of the structure factor as a function of temperature is found.

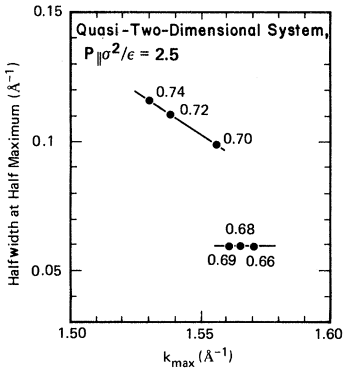

FIG. 19. Halfwidth at half maximum of the first peak of the atomic structure factor vs peak position for various temperatures indicated at the experimental points. The results are for the *quasi*-two-dimensional system of 576 atoms at $P^*_{\|}=2.5$.

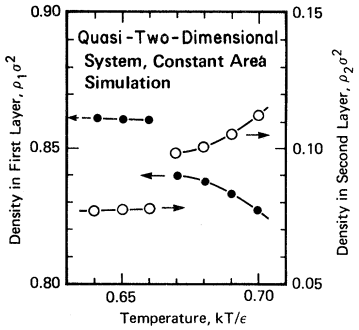

FIG. 20. Effective two-dimensional density in the first layer (left scale) and in the second layer (right scale) vs temperature for the *quasi*-two-dimensional constant-area simulations.

B. Constant-area simulations

We have already remarked that, for a strictly two-dimensional atomic system that has first-order phase transitions, it is possible to simulate two-phase coexistence if the density is held fixed and the system is in the appropriate region of the phase diagram. This has been confirmed for the two-dimensional Lennard-Jones system.[12] We now demonstrate that, for sufficiently high temperatures and pressures where second-layer population is likely, two-phase coexistence is not possible since the second layer acts as an atom reservoir for the first-layer, high-density subsystem. In Fig. 20 the first- and second-layer densities are presented. By equilibrating the system at a temperature of 0.70 and an area $A^*=A/\sigma^2=612.5$, a fluid phase is established in the first layer with a density of 0.827. The fluid phase remains as the system's temperature is decreased with accompanying monotomically increasing density until, at a temperature $T^*=0.66$, the first-layer atoms solidify and the density increases discontinuously to 0.86. Of course, this is accompanied by a discontinuous decrease of the second-layer density due to the conservation of the total number of xenon atoms. This scenario is displayed in Fig. 21 where trajectory pictures for the various temperatures are shown. Thus contrary to a strictly two-dimensional system, this two-layer system cannot support two-phase coexistence. However, for conditions where only the first layer is populated, two-phase coexistence may occur; we have simulated it but do not show it here.

V. SUMMARY AND RELATION OF THE SIMULATION RESULTS TO THE EXPERIMENT OF HEINEY *et al.*

First, we dealt with certain issues concerning the legitimacy of using computer-simulation experi-

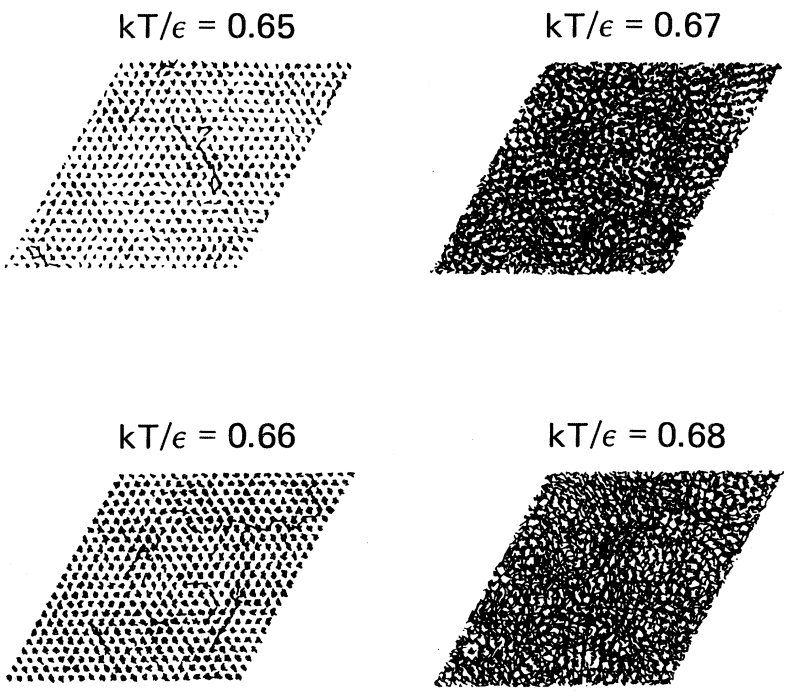

FIG. 21. Trajectory pictures of the equilibrium state in the first layer for the *quasi*-two-dimensional constant-area simulations at various temperatures. Note that there is no two-phase coexistence.

ments for studying phase transitions in two-dimensional systems. We hope that our discussion was convincing. Then, we presented a rather extensive set of computer experiments on the thermodynamics and structure of xenon adsorbed on graphite. The portion of the phase diagram studied was governed by our interest in comparing our findings to the recent laboratory experiment of Heiney *et al.*,[20] which is at odds with lower-coverage laboratory experiments and with the two-dimensional computer simulations. In particular, Heiney *et al.* interpreted their results as indicating the freezing transition to be continuous with fluid correlation lengths exceeding 100 atomic spacings for a coverage of 1.1 monolayers and for a reduced temperature of approximately 0.7. We were particularly interested in investigating any influence of the *third dimension of freedom* on the order of the freezing transition for a *quasi*-two-dimensional system at high coverages and temperatures. We made several simulations in this pressure-temperature regime in question, knowing that the two-dimensional Lennard-Jones phase diagram predicts a first-order liquid-solid transition, yet anticipating possible new physics associated with *second-layer promotion.* While we reported many interesting features resulting from an intimate interaction between the first and second adsorption layers, we found that the character of the freezing transition did not change; the transition is clearly first-order, and the phase diagram closely corresponding to the phase diagram of a strictly two-dimensional system. We conclude that, compared to an idealized two-dimensional system of simple atoms, the third dimension associated with xenon adsorbed on graphite changes the details of the liquid-solid transition, but the main result, the first-order nature of the phase transition, remains valid.

*Permanent address: Institut für Theoretische Physik, Universität Frankfurt, Frankfurt, West Germany.

[1]O. E. Vilches, Annu. Rev. Phys. Chem. 31, 463 (1980).

[2]D. Frenkel and J. P. McTague, Annu. Rev. Phys. Chem. 31, 491 (1980).

[3]J. E. Lane and T. Spurling, Aust. J. Chem. 31, 933 (1978).

[4]F. Hanson and J. P. McTague, J. Chem. Phys. 72, 6363 (1980).

[5]D. Henderson and P. J. Leonard, in *Physical Chemistry: An Advance Treatise,* edited by H. Eyring, D. Henderson, and W. Jost (Academic, New York, 1971), Vol. VII B, p. 413.

[6]W. A. Steele, Surf. Sci. 36, 317 (1973).

[7]R. W. Hockney and J. W. Eastwood, *Computer Simulation Using Particles* (McGraw-Hill, New York, 1981), Sec. 8-4.

[8]D. R. Dion, J. A. Barker, and R. P. Merrill, Chem. Phys. Lett. 57, 298 (1978).

[9]Farid F. Abraham, Rep. Prog. Phys. 45, 1113 (1982).

[10]N. Metropolis, A. W. Rosenbluth, M. N. Rosenbluth, A. H. Teller, and E. Teller, J. Chem. Phys. 21, 1087 (1953).

[11]A. Rahman, Phys. Rev. A 136, 405 (1964).

[12]F. F. Abraham, Phys. Rep. 80, 339 (1981).

[13]A. D. Novaco and P. A. Shea, Phys. Rev. B 26, 284 (1982).

[14]J. A. Barker, D. Henderson, and F. F. Abraham, Physica (Utrecht) 106A, 226 (1981).

[15]H. Müller-Krumbhaar and K. Binder, J. Stat. Phys. 8, 1 (1973); Phys. Rev. B 7, 3300 (1973).

[16]W. G. Hoover, W. T. Ashurst, and R. J. Olness, J. Chem. Phys. 60, 4043 (1974).

[17]S. Toxvaerd (unpublished).

[18]F. A. Lindemann, Z. Phys. 11, 609 (1910).

[19]P. Dutta and S. K. Sinha, Phys. Rev. Lett. 47, 50 (1981).

[20]P. A. Heiney, R. J. Birgeneau, G. S. Brown, P. M. Horn, D. E. Moncton, and P. W. Stephens, Phys. Rev. Lett. 48, 104 (1982).